Journal of Basic and Environmental Sciences

ISSN
Online:2356-6388
Print:2536-9202

Research Paper Open Access

A prospective chitosan produced from a biological source: Extraction, Characterization, and Assessment of biological performance

Fatma K. Mohamed[a], Fatma N. El-Shall[b], Mohamed E. EL Awady[c], Mohamed H. Yassin[a], Ghada E. Dawwam[a]

[a]Botany and Microbiology Department, Faculty of Science, Benha University, Benha 13518, Egypt
[b] Dyeing, Printing and Textile Auxiliary Department, National Research Centre, 33 El-Buhouth St., Dokki, Giza P.O. 12622, Egypt.
[c] Microbial Biotechnology Department, Biotechnology Research Institute, National Research Centre, 33 El-Buhouth St., Dokki, Giza P.O. 12622, Egypt.
Corresponding author: ghada.ibrahem@fsc.bu.edu.eg. https://orcid.org/0000-0002-2911 658X.

Abstract

Chitosan, a biodegradable and biocompatible biomaterial, was extracted alongside chitin from Black Soldier Fly Pupae (BSFP). In our study, chitin and chitosan were extracted from Black Soldier Fly (BSF) and assessed for their biomedical applications. Characterization was performed using ATR-FTIR, XRD, and UV–Vis spectroscopy. The chitin content accounted for approximately 36.8% of the pupal dry mass. Extracted chitosan exhibited notable biological activities: moderate antibacterial and antifungal effects against *Bacillus subtilis* ATCC-6633, *Staphylococcus aureus* NRRLB-767, *Escherichia coli* ATCC-25922, *Pseudomonas aeruginosa* ATCC-10145, *Candida albicans* ATCC-10231, and *Aspergillus niger* NRRLA-326, significant antioxidant properties (e.g., 36.98% 2,2-diphenyl-1-picrylhydrazyl (DPPH) and 31.33% 2,2′-azino-bis (3-ethylbenzothiazoline-6-sulfonic acid (ABTS) radical scavenging at 500 µg/ml), and metal ion chelation (30.83%). It inhibited lipid peroxidation (35.39%) and demonstrated free radical scavenging activity (SOR: 38.28%, NO: 26.40%). Anti-inflammatory assays showed inhibition of COX-1 (50.20%) and COX-2 (49.61%). Additionally, chitosan showed cytotoxicity against several cancer cell lines (Wi-38, HepG2, CaCo-2, and A549) with IC_{50} values ranging from 19.36 to 41.17 µg/ml. Thus, these results support the potential of chitosan as an antimicrobial, anti-inflammatory, and anticancer agent.

Keywords: *Chitin, Chitosan, Black Soldier Fly, Antimicrobial activity, Antioxidant activity, cytocompatibility.*

Submit Date 2025-06-24
Accept Date 2025-07-1
Published Date 2025-07-31
Doi: 10.21608/jbes.2025.396559.1023

1. Introduction

The emergence and dissemination of antibiotic-resistant organisms pose significant health risks even to individuals who have not been directly exposed to specific antibiotics. This growing threat highlights the pressing demand for novel antibacterial agents capable of effectively combating infections that no longer respond to conventional treatments [1].

Antibiotic resistance in bacteria is responsible for hundreds of thousands of deaths annually, posing an escalating global health concern. The rapid proliferation of strains resistant to widely used antibiotics—including those considered last-resort treatments—intensifies this crisis. The swift global transmission of resistance genes underscores the urgency of the situation and calls for coordinated international efforts to address the growing prevalence of multidrug-resistant bacterial populations [2].

Chitosan refers to a group of linear polysaccharides consisting of varying proportions of (β1→4)-linked units of N-acetyl-D-glucosamine and D-glucosamine. This biopolymer is naturally found in a wide range of organisms, including the exoskeletons of crustaceans (e.g., lobsters, shrimp, krill, barnacles, crayfish), mollusks (e.g., octopus, cuttlefish, clams, oysters, squids, snails), various algae (e.g., diatoms, brown and green algae), insects (e.g., houseflies, silkworms, ants, cockroaches, spiders, beetles, scorpions, brachiopods), and the cell walls of fungi such as those belonging to Ascomycetes, Basidiomycetes, and Phycomycetes—including species like *Aspergillus niger*, *Mucor rouxii*, *Penicillium notatum*, and *Trichoderma reesei* [3].

Hamed et al. [4] demonstrated the efficient isolation of chitin from both pupal shells and adult black soldier flies (BSF) using demineralization, deproteinization, and decolorization methods. Chitosan is subsequently synthesized from chitin through a sequence of chemical processes, primarily involving demineralization, deproteinization, and deacetylation. While decolorization is sometimes included, it is generally considered a minor step. Chitin can be sourced either from purified synthetic materials or extracted from various natural origins. According to Thambiliyagodage et al. [5], shrimp shells are among the most common sources, along

with crab shells and certain fungi. Prior to chemical processing, shrimp shells are thoroughly washed, dried, and ground to eliminate contaminants. These shells are composed of chitin, proteins, and inorganic minerals like calcium carbonate and calcium phosphate, which are intricately bound within the exoskeletal matrix.

Chitosan is a biodegradable, biocompatible, and non-toxic biopolymer widely utilized across various sectors, including agriculture, pharmaceuticals, medicine, food production, and textiles. In recent years, emerging applications in biomedicine, biotechnology, wastewater treatment, catalysis, packaging, and bioimaging have highlighted its potential to contribute to a more sustainable future—thanks to its versatility, recyclability, and cost-effectiveness [6].

"Chitosan, along with its derivatives and chitooligosaccharides, exhibits antimicrobial effects against a broad spectrum of microorganisms, including bacteria, filamentous fungi, and yeasts. These compounds appear to inhibit microbial growth, as evidenced by the resumption of bacterial proliferation once chitosan is removed from the environment [7].

Chitosan contains amino and multiple hydroxyl groups capable of interacting with free radicals, giving it notable free-radical scavenging properties. Certain derivatives—such as chitosan sulfates and N-2-carboxyethyl chitosan—have demonstrated enhanced antioxidant activity [8].

Inflammation is a natural physiological response triggered by tissue injury or infection, primarily aimed at directing circulating leukocytes and plasma proteins to the affected site to eliminate harmful agents and initiate repair. This process is closely linked to the generation of free radicals. Interestingly, lower molecular weight forms of chitosan, particularly Chito-oligosaccharides, appear to exhibit more pronounced antioxidant effects in these contexts [9].

Chitosan is significant across various medical fields, particularly in periodontal and orthopedic drug delivery, wound healing, and tissue engineering. Its applications extend to surgical sutures, contact lenses, ophthalmic solutions, artificial skin and blood vessels, bandages, sponges, burn dressings, antitumor and antiviral agents, bone regeneration materials, and hemostatic products [10].

Due to its strong chelating capacity and multifunctional properties, chitosan is also widely employed in the food industry. It serves in the removal of unwanted substances—such as dyes, fats, and particulate matter—and functions as a natural and safe preservative, particularly in

the United States, where it supports extended food shelf-life [11].

Chitosan is extensively utilized in drug delivery systems due to its biocompatibility and functional versatility. It supports multiple administration routes—including oral, ocular, and transdermal—depending on specific therapeutic needs. Notably, oral drug delivery involving chitosan has shown promising outcomes, particularly through pH-responsive drug release mechanisms that enhance targeting of specific absorption sites. Beyond its role as a drug carrier, chitosan can also be administered independently for health benefits. Studies have demonstrated that low-molecular-weight chitosan contributes to reduced cholesterol and triglyceride levels, thereby lowering the risk of cardiovascular disease. This effect is likely due to electrostatic interactions between positively charged chitosan molecules and negatively charged fatty acids and bile salts [12].

Among its many advantages, chitosan stands out as a natural cationic polymer—an uncommon feature among polysaccharides, which are typically neutral or anionic. This positive charge enables the formation of multilayer assemblies or electrostatic complexes when combined with synthetic or anionic natural polymers, broadening its potential in advanced materials and biomedical applications [13].

This study aimed to extract and characterize chitin and chitosan from the pupal stage of the Black Soldier Fly, and to evaluate the biological properties of the produced chitosan. Characterization techniques included ATR-FTIR spectroscopy, X-ray diffraction (XRD), and UV–Vis spectrophotometry. The biological evaluation encompassed antimicrobial, antioxidant, anti-inflammatory, and cytocompatibility assays to assess the potential of insect-derived chitosan as a multifunctional biomaterial for biomedical and pharmaceutical applications.

2. Materials and Methods

2.1. Chitin extraction

The black soldier fly was kindly provided from a local farm. According to the results published by Soetemans, Uyttebroek et al. [14], the researchers examined chitin collected and generated during various phases of the Black Soldier Fly (BSF) life cycle **(Figure 1)**. The pupae stage (BSFP) had a substantial amount of chitin, which will be used for chitin production in this study. The extraction of chitin from black soldier fly pupa waste residue (BSFP) was conducted using the technique described by Rodríguez et al. [15]. The insect remnants were crushed, dried in an air-circulating oven, and then stored in the freezer for future use.

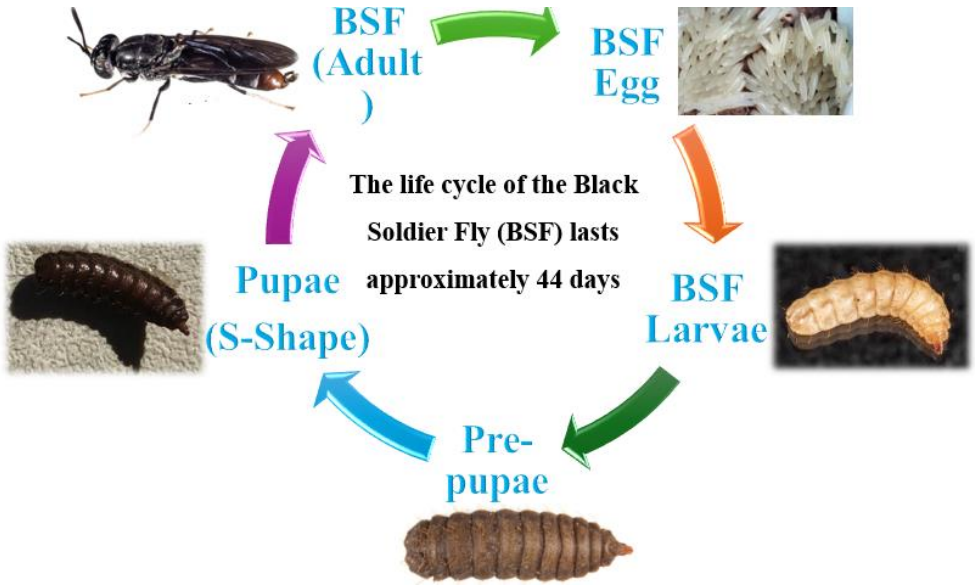

Figure 1: The life cycle of black soldier fly.

The chitin extraction approach consisted of the following steps: defatting, demineralization, deproteinization, and subsequently depigmentation, as illustrated in **Figure 2.**

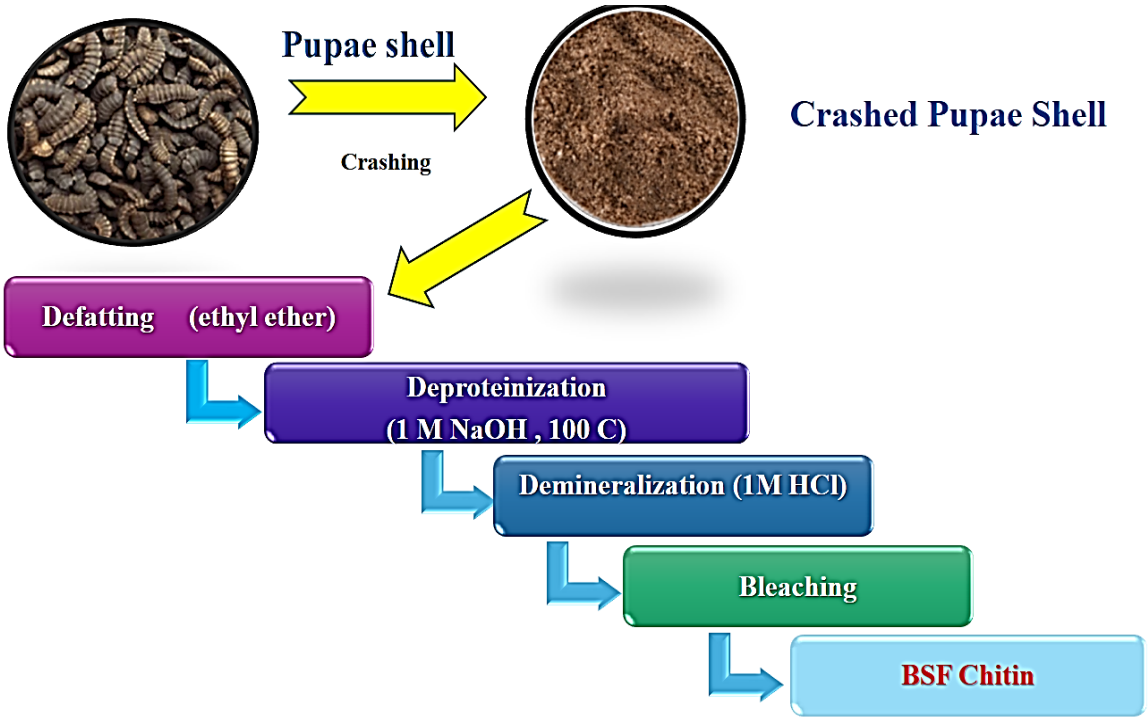

Figure 2: The process of converting black soldier fly's pupa (BSFP) into chitin.

- For defatting. Petroleum ether was employed in a Soxhlet extraction system to separate lipids and fats. The reaction finished when the ether solvent employed in the Soxhlet extractor became clear. After defatting, the sample was dried in an air circulation oven. The sample was then stored in the refrigerator for further reuse.
- For demineralization, 5 g of the sample was suspended: liquid ratio of 1:10 (m/v) in 1 M HCl at ambient temperature for 1 hour to remove minerals.
- Sample was rinsed with distilled water until neutral pH was established.
- For deproteinization, the dried demineralized sample had been treated with NaOH (1 M) at 80°C and 200 rpm for 1 hour at a liquor ratio of 1:25 (m/v). This step was repeated about six times before being washed with HCl (1 M) and distilled water until neutral pH was restored.
- For depigmentation of the extracted chitin sample, 50 ml of 12% H_2O_2 was added to the demineralized and deproteinized sample and stirred at 250 rpm at 80°C. The pH was subsequently adjusted to 12 using NaOH.
- Subsequently, the sample was then filtered via filter paper. The dried chitin sample was weighed to calculate the yield using Eq. (1).

$$\text{Yield \% (Chitin)} = \text{Mass of Chitin} / (\text{Insect mass}) \times 100 \quad (1)$$

2.2. Chitosan extraction

BSF chitosan was generated from a BSFP chitin sample using a modified approach of the technique reported by Yuan et al. [16] **(Figure 3)**. One gram of previously separated BSFP chitin was deacetylated with 50% NaOH at a solid: liquid ratio of 1:30 (m/v) for 8 hours at 90°C and 300 rpm. The process was repeated three to five times. The sample was filtered, rinsed with distilled water till neutral pH, and then dried.

The percentage of chitosan yield was calculated in accordance with equation 2.

$$\text{Yelid of Chitosan \%} = \frac{\text{Mass of Extracted Chitosan}}{\text{Mass of Chitin}} \quad (\mathbf{2})$$

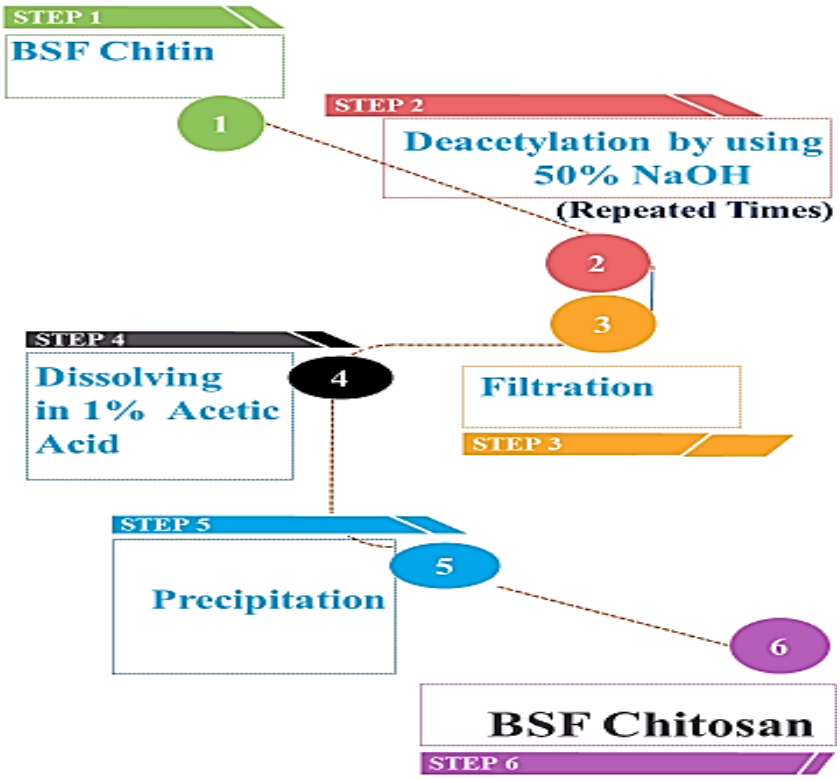

Figure 3. Schematic representation illustrating the process of extracting chitosan from the chitin of black soldier fly's pupa (BSFP).

2.3. Characterization

ATR-FTIR spectra of the samples were scanned on a JASCO FT-IR 6100 spectrometer (Tokyo, Japan), the measurements were conducted between the ranges of 400 and 4000 cm^{-1}, with 60 scans and a resolution of 4 cm^{-1}.

X-ray diffraction (XRD) analysis was done for extracted chitin and chitosan using a Panalytical Empyrean X-ray diffractometer (PANalytical, Netherlands). The machine was operated at 40 kV and, 15 mA using Cu-Kα radiation (1.54056 Å). The X-ray diffractogram was recorded in the range 10 – 80º (2θ) with a step size of 0.015º, and a scan speed/duration of 10.0º /min. UV–Vis spectrophotometer measurements were carried out by JASCO V-730 UV–visible/NIR double-beam spectrophotometer, Tokyo, Japan. The crystalline index (CI) was determined by equation 3:

$$\mathbf{CI} = \frac{\mathbf{I_{110} - I_{AMR}}}{\mathbf{I_{110}}} \times \mathbf{100} \qquad (\mathbf{3})$$

where I_{am} is the intensity of amorphous diffraction and I_{110} is the greatest intensity at $2\theta = 20^{\circ}$.

2.4. Bioactivity of chitosan

2.4.1. Assessment of antimicrobial activity

To evaluate chitosan's antibacterial potential, assays were performed using flat-bottom 96-well polystyrene microplates.

The selected test organisms included *Bacillus subtilis* ATCC-6633, *Staphylococcus aureus* NRRLB-767, *Escherichia coli* ATCC-25922, *Pseudomonas aeruginosa* ATCC-10145, *Candida albicans* ATCC-10231, and *Aspergillus niger* NRRLA-326. After an incubation period of approximately 20 hours, optical density at 600 nm (OD600) was measured with a Spectrostar Nano Microplate Reader (BMG LABTECH GmbH, Allmendgrün, Germany), and results were expressed as mean values with standard deviation (SD) [17].

2.4.2. Assessment of chitosan antioxidant activity

2.4.2.1. DPPH free radical scavenging activity

As the Brand Williams, *et al.,* [18]**,** The scavenging activity of the DPPH radical was assessed as follows: Scavenging rate (%) = $[(A_{control} - A_{sample}) / A_{control}] \times 100$

2.4.2.2. ABTS scavenging activity

According to technique outlined by Miller & Rice-Evans, [19], The following calculation was carried out to determine the ABTS radical cation scavenging activity as determined in equation 4.

ABTS activity (%) = $[(A_{control} - A_{sample}) / A_{control}] \times 100$ **(4)**

2.4.2.3. Ferrous reducing antioxidant capacity assay

By using the Oyaizu technique [20], The reaction mixture's enhanced reducing power is indicated by its increased absorbance. At each concentration, the experiment was carried out three times.

2.4.2.4. Lipid peroxidation inhibition assay

The lipid peroxidation inhibition assay was conducted according to [21]**.** The lipid peroxidation inhibition was determined in equation 5:

$$\% \text{ Lipid peroxidation inhibition} = [(\text{Acontrol} - \text{Asample})/\text{Acontrol} \times 100] \quad (5)$$

2.4.2.5. Superoxide radical scavenging activity

In accordance with the established methodology [22], The proportion of superoxide radical scavenging was determined by the formula at equation 6:

$$\text{Activity (\%)} = [(A_{control} - A_{sample})/A_{control} \times 100] \quad (6)$$

2.4.2.6. Nitric oxide scavenging activity

According to the procedure outlined by Adithya et al. [23], The absorbance was quantified at 540 nm.

2.5. Evaluation of anti-inflammatory activity by cyclo-oxygenase enzymes (COX-1 & COX-2)

The inhibitory activity with respect to assess cyclooxygenase-1 (COX-1) and cyclooxygenase-2 (COX-2) according to the method of Lee et al. [24]. The percentage of COX inhibition was assessed as determined in equation 7:

$$\text{COX inhibition activity (\%)} = (\text{AIAS} - \text{ASP})/\text{AIAS} \times 100 \quad (7)$$

Where AIAS is the absorbance of the 100% starting activity and ASP is the absorbance of the inhibitor sample.

2.6. Cytocompatibility assay

Cell lines for human diploid fibroblast cell line (WI-38), human hepatocellular carcinoma (HepG2), colorectal adenocarcinoma (CaCo-2), lung adenocarcinoma (A-549) were tested to determine the cytotoxicity assay. The MTT viability test was used to assess according to Mosmann [25]. The following formula was used to determine cell viability:

$$\text{Viability \%} = \frac{\text{Test OD}}{\text{Control OD}} X\ 100 \quad \text{Equ. (8)}$$

3. Results and discussion

Through applying Equation 1 to calculate the BFP's chitin yield, it was revealed that the content percentage is similar to 36.8% of the total dry mass of the black soldier fly pupa. Characterizing the extracted chitin is critical for determining their suitability for certain applications. The resultant yield appears to be higher than those from other sources [14, 26–28].

The FTIR spectra of the chitin that was extracted from PSFP are shown in **Figure (4)**. Three amide peaks characteristic of the chitin were identified in the IR spectra. These peaks are located at 1620 cm^{-1} for C-O (amide I), 1551 cm^{-1} for N-H (amide II), and 1308 cm^{-1} for C-N (amide III) [16]. The distinct peaks observed can indicate the presence of chitin in the provided spectrum [29]. Furthermore, O-H and N-H asymmetric stretching is shown by the peak in the chitin spectrum at 3254 cm^{-1} [30]. Moreover, the distinct pattern in the FTIR spectrum allows for the differentiation of α-chitin from its other crystalline forms, such as β- and γ-chitin, which show a shift in these peaks due to variations in hydrogen bonding interactions. The α-chitin form displays two peaks that suggest the presence of hydrogen bonds. One peak corresponds to an intramolecular bond between the carbonyl group and the $-CH_2OH$ group at 1620 cm^{-1}, while the other indicates an intermolecular bond between the NH group and the carbonyl group at 1655 cm^{-1}. Based on the results, the chitin recovered from BSFP could be categorized as α-type [14, 16]. This particular type of chitin is typically found in tough structures, including insect cuticles [30].

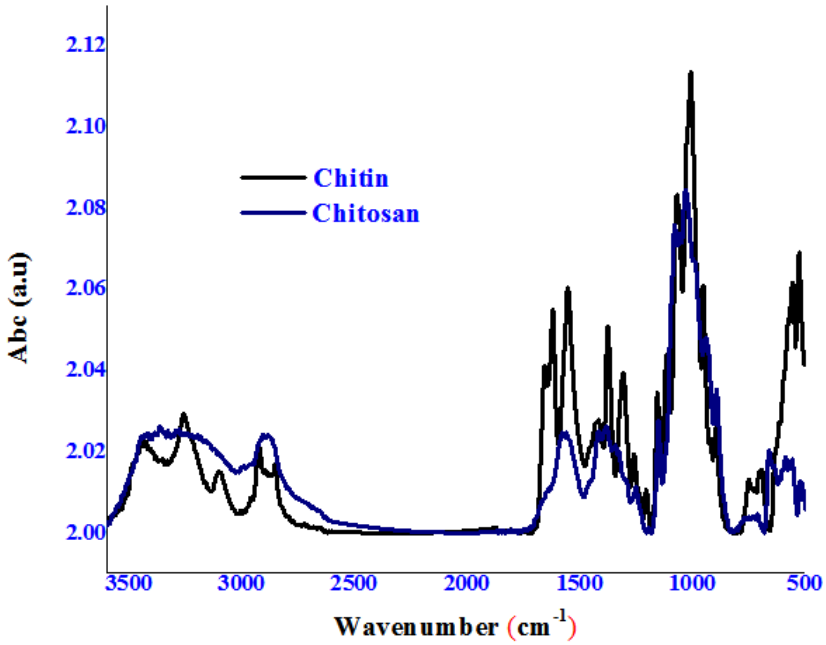

. **Figure 4.** ATR-FTIR spectra of extracted BSFP chitin and chitosan

In **Figure 4**, the FTIR spectrum of chitosan derived from BSFP chitin shows a wide band at 3000-3600 cm^{-1}, indicating stretching vibration of O-H and N-H bonds. Also, there is a band at about 2929 cm^{-1}, known to be for stretching vibration -CH_2, found in the CH_2OH unit [31]. A distinct spectrum area between 1500 and 1700 cm^{-1} is commonly used to distinguish between chitosan and chitin. The less intense signal corresponding to amide C--O indicates that chitin deacetylation has actually occurred [32]. The position shifts and intensity reduction of the signal corresponding to amide C--O suggest that chitin deacetylation has actually occurred. Stretching vibrations corresponding to C=O, N-H, C-N, C-O, C-O, and C-H bonds are represented by specific peaks at 1629 cm^{-1}, 1539 cm^{-1}, 1399 cm^{-1}, 1152 cm^{-1}, 1071 cm^{-1}, 1013 cm^{-1}, and 643 cm^{-1} [33].

One key factor influencing chitosan's biological and physicochemical properties, along with its potential applications, is its degree of deacetylation (DD). The molar proportion of monomeric glucosamine units in chitin is indicated by the deacetylation degree (DD) value, which can range from 0 to 100. The DD in chitosan increases with the number of deacetylated groups present in the chitin structure [34]. Chitosan is available in different levels of purity and degree of deacetylation, based on use [30]. The degree of deacetylation (DDA) was determined using an infrared spectroscopy method [35]. It was estimated based on the following formulae (equation 9):

$$\mathrm{DD}(\%) = \frac{[(A_{1320}|A_{1420}) - 0.3822]}{0.03133} \qquad (9)$$

$$\mathrm{DDA} = 100 - \mathrm{DA}(\%)$$

Where, A1320 refers to the absorbance at the peak area corresponding to the band at 1320 cm^{-1}, while A1420 refers to the absorbance at the peak area for the band at 1420 cm^{-1}. DDA denotes the degree of deacetylation percentage, and DA indicates the degree of acetylation. The calculation yielded a DDA value of 80.34%. The result is consistent with previous studies on the topic [35].

The percentage of BSFP chitin to chitosan conversion was also determined using Equation 2. The content percentage has been determined to be comparable to 6.35% of the BSFP chitin's total dry mass [28].

Figure (5) represents the XRD pattern of isolated BSFP chitin and chitosan. XRD diffractograms highlight structural characteristics of chitin and chitosan samples, indicating their α-form. A more amorphous or less organized arrangement of the polymer chains in these samples is suggested by the less strong peaks seen at 9° and 10°. Understanding these peaks is critical for applications in materials science and healthcare since structural variation may significantly affect mechanical strength and solubility.

Moreover, the distinctive peaks at 19° and 19.5° highlight the crystalline regions found in chitin and chitosan, which contribute to their stability and functioning over a wide variety of circumstances. The small peaks at 23°,25°,27° for chitin and 21.5 for chitosan was also observed [36].

Significant variations between isolated chitin and chitosan were found when the CI was calculated from the XRD data. CI of chitin found to be 76.8%, while CI of chitosan calculated to be 65.4%. Chitin is usually considered to be more crystalline than chitosan. This is because chitin retains more of its original structure. Chitosan, on the other hand, is more amorphous and has increased flexibility and water solubility due to the presence of deacetylated amino groups [37]. The chitin crystallinity index (CI) levels for crab and insect chitin range from 40% to 90%, with a typical range of 60% to 80%. This variation is influenced by several factors, including species, source, growth stage, gender, and the purification technique [36].

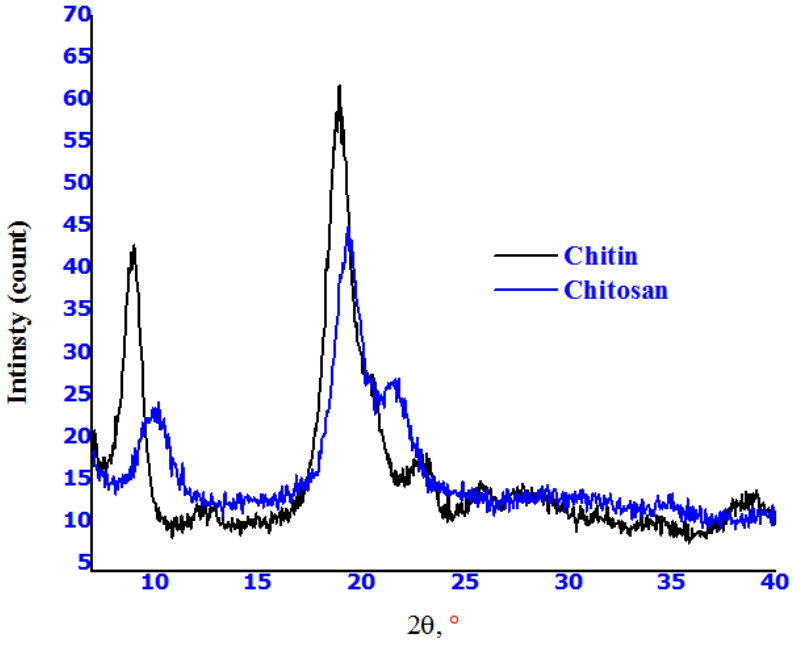

Figure 5. XRD diffractograms of extracted BSFP chitin and chitosan

Figure (6) illustrated the UV-vis spectrum of chitosan sample (dissolved in 1% acetic acid) extracted from BSFP chitin. The UV-vis spectrum of a chitosan sample that was separated from BSFP chitin and dissolved in 1% acetic acid is illustrated in **Figure 6.** According to the **figure 6**, the chitosan spectrum shows an appropriate absorption band at 292 nm, which is related to the existence of the π-π* transition of its C=O group in the chitosan structure (Soret band.). This finding is in good agreement with the cited data [38].

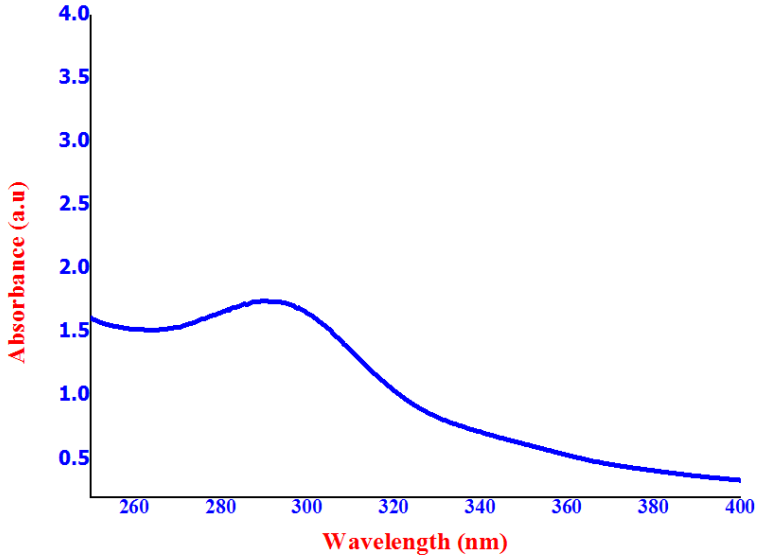

Figure 6. UV-vis spectrum of extracted chitosan

Antimicrobial activity of chitosan

Chitosan has moderate antibacterial effects against *Staphylococcus aureus* NRRLB-767 and *Bacillus subtilis* ATCC-6633 with 15.85±0.94 and 17.79±1.00, respectively. In addition, antibacterial effects were high against *Escherichia coli* ATCC-25922 and *Pseudomonas aeruginosa* ATCC-10145 with 19.94±0.89 and 20.69±0.85, respectively. While, it has antifungal against *Candida albicans* ATCC-10231 and *Aspergillus niger* NRRLA-326 with 13.68±0.85 and 20.86±0.6 as shown in **Table 1**. Chitosan can inhibit the proliferation of many bacteria, fungi, and yeasts, with different mechanisms, not all fully clarified [39]. The simplest mechanism of action involves electrostatic interactions between the NH_3^+ sites of chitosan (positively charged) and the membranes of microbial cells (negatively charged).

Due to its limited ability to penetrate microbial cell walls and membranes, high-molecular-weight chitosan exerts its antimicrobial activity primarily through alternative mechanisms. These include chelating essential metal ions, which disrupts nutrient uptake at the extracellular level, and compromising cell membrane integrity by altering its permeability [40]. This disruption facilitates the leakage of intracellular contents [41]. Furthermore, research by Chung and Chen [42] demonstrated that chitosan binds to microbial enzymes and nucleotides, ultimately leading to structural damage in organisms such as *Escherichia coli* and *Staphylococcus aureus*.

Table 1. Antimicrobial activity of chitosan

	Staph. aureus NRRLB-767	*B. subtilis* ATCC-6633	*P. aeruginosa* ATCC-10145	*E. coli* ATCC-25922	*C. albicans* ATCC-10231	*A. niger* NRRLA-326
Chitosan	15.85 ± 0.94	17.79 ± 1.00	20.69 ± 0.85	19.94 ± 0.89	13.68 ± 0.85	20.86 ± 0.63
Ciprofloxacin	96.85 ± 0.53	91.27 ± 0.81	98.45 ± 0.18	96.76 ± 0.92	-ve	-ve
Nystatin.	-ve	-ve	-ve	-ve	96.85 ± 0.34	96.28 ± 0.83

Antioxidant activity of chitosan

The quantitative assessment of antioxidant scavenging activity was conducted at various concentrations from 100 - 500 µg/ml **(Table 2)**. The maximum antioxidant activity of chitosan (500 µg/ml) was 36.98±0.64 % for DPPH scavenging activity. While, ABTS radicals scavenging activity of 31.33±1.09%. To assess the chelating efficiency of chitosan, the chelation of ferrous ions (Fe^+) exhibited a

chelating percentage of 30.83±0.38% at (500 µg/ml).

Chitosan prevented the peroxidation of linoleic acid (35.39±0.94%) seen at concentration (500 µg/ml). Chitosan exhibited SOR scavenging percentage 38.28±0.19% at 500 µg/ml. Also, the NO radical scavenging capacity of chitosan was assessed by NO system with 26.40±1.08% at the maximum dosage of 500 µg/ml.

Chitosan is widely recognized for its antioxidant properties, which has drawn considerable interest from researchers across diverse scientific disciplines [43], many *in vitro* and *in vivo* studies have shown that chitosan exhibits redox-regulatory activity due to inhibition of ROS production, prevention of lipid oxidation by significantly reduced serum free fatty acids, and malondialdehyde concentrations and increases intracellular antioxidant enzymes in biological systems.

Santhosh et al. [44] reported that chitosan effectively prevented lipid peroxidation in the livers of rats exposed to hepatotoxic agents such as isoniazid and rifampicin. Similarly, Wen et al. conducted a comparative study evaluating the effects of chitosan, chitosan nanoparticles, and vitamin C on the activation of intracellular antioxidant enzymes in the RAW264.7 mouse macrophage cell line. Their findings indicated that exposure to 500 µM hydrogen peroxide (H_2O_2) for 12 hours significantly reduced the activities of superoxide dismutase (SOD) and glutathione (GSH). However, pre-treatment with chitosan nanoparticles at a concentration of 100 µg/mL effectively restored enzyme activity. Notably, chitosan nanoparticles exhibited greater restorative effects on SOD and GSH than standard chitosan, with antioxidant recovery levels nearly matching those induced by vitamin C at 250 µM/mL. The study attributed this protective effect to enhanced expression and activity of endogenous antioxidant systems in response to the nanoparticles [44].

Table 2. Antioxidant activity of chitosan

Concentrations (µg/ml)	DPPH	ABTS	Fe	No	Lipid	O
100	20.56±0.61	19.83±0.57	19.86±0.54	18.78±0.34	25.66±0.40	21.04±0.27
200	23.95±0.90	22.41±1.02	22.71±0.90	20.82±0.46	29.49±0.50	24.22±0.49
300	29.15±0.65	27.03±0.78	25.65±0.86	22.87±0.56	31.45±0.67	29.18±0.32
400	31.71±0.97	28.78±0.56	27.94±0.66	23.60±0.51	32.64±0.42	34.19±0.82
500	36.98±0.64	31.33±1.09	30.83±0.38	26.40±1.08	35.39±0.94	38.28±0.19

Anti-inflammatory activity of Chitosan

The anti-inflammatory activity was assessed through various methods as cyclooxygenase (COX1) inhibitory that showed the Inhibition percentage (%) was 50.20±0.69 %, while the cyclooxygenase (COX2) inhibitory provided 49.61±0.73 % at 500 µg/ml **(Table 3).**

Chitosan exhibits immunomodulatory properties, including the suppression of pro-inflammatory cytokines and the stimulation of tissue granulation through fibroblast recruitment [45]. Collectively, these effects highlight its potential as an antimicrobial agent, anti-inflammatory compound, and promoter of wound healing.

However, while gaining a polycationic charge in a weakly acidic environment such as one supported by the epidermis, chitosan is weakly soluble in physiologic solvents, therefore limiting its clinical use to date [46].

Table 3. Anti-inflammatory activity of chitosan

Concentration (µg/ml)	COX1	COX2
100	40.76±0.47	38.36±0.21
200	42.71±0.89	40.99±0.59
300	45.92±0.49	43.82±0.78
400	46.90±0.70	45.80±0.66
500	50.20±0.69	49.61±0.73

Antitumor activity against different cell lines

Antitumor activity was evaluated by the MTT viability/cytotoxicity method against Wi-38, HepG2, CaCo-2, and A549 cell lines. IC_{50} value was calculated to be 41.17 ± 0.52, 19.36 ± 0.18, 22.53 ± 0.31, and 27.99 ± 0.22 µg/ml for cell lines Wi-38, HepG2, CaCo-2, and A549 cell lines, respectively, as shown in **Figure 7.**

Through chemical modification, a variety of chitosan derivatives with enhanced solubility and broad applicability can be synthesized. These modifications—primarily targeting the amino and acetamido groups—have been shown to improve both solubility and biological activity. One example is 2-phenylhydrazine (or hydrazine) thiosemicarbazone chitosan, whose cytotoxic effects are associated with its antioxidant capacity to neutralize carcinogenic free radicals. The oxidative stress generated by an imbalance between reactive oxygen species and antioxidant defenses is considered a key contributor to cancer development. Additionally, chitosan-

metal complexes demonstrate antitumor potential through interactions with DNA and their free radical scavenging properties. Various derivatives, including carboxymethyl chitosan (CMCS), chitosan–thymine conjugates, sulfated chitosan (SCS), sulfated benzaldehyde chitosan (SBCS), glycol chitosan (GChi), N-succinyl chitosan (Suc-Chi), furanoallocolchicinoid-chitosan conjugates, and polypyrrole–chitosan hybrids, have all been reported to exert antitumor effects via distinct apoptotic pathways [47].

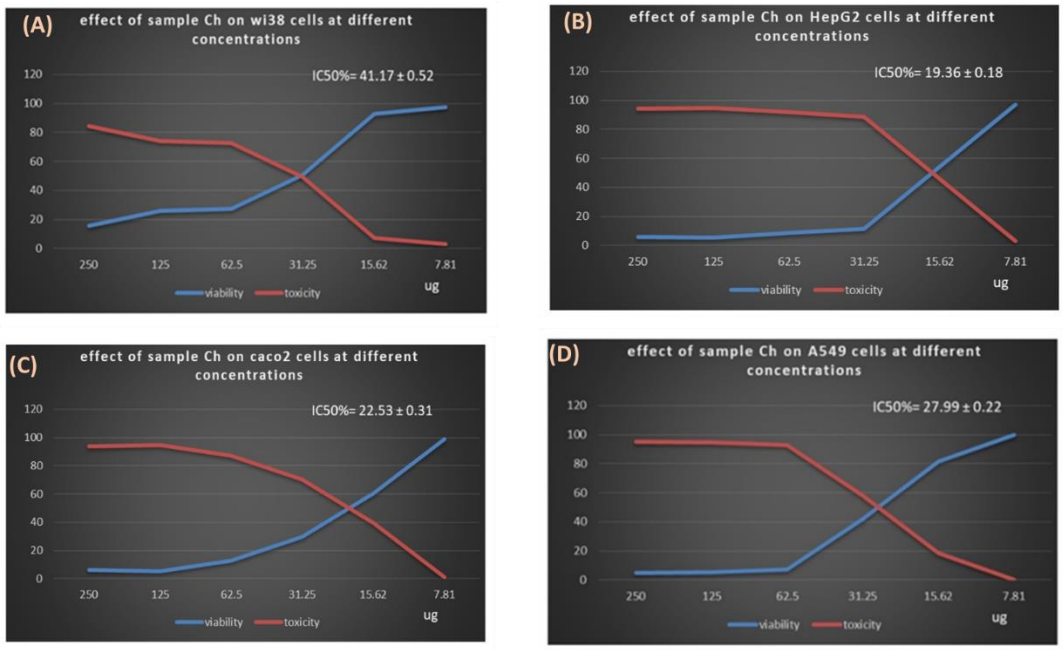

Figure 7: Antitumor activity of chitosan against different (A) Wi-38, (B) HepG2, (C) CaCo-2, and (D) A549 cell lines.

4. Conclusion

The extraction of chitin and chitosan from the pupa stage of Black Soldier Fly provides a sustainable and promising biomaterial source. The comprehensive physicochemical characterization confirmed the successful isolation of high-quality chitin and its conversion to chitosan, yielding approximately 36.8% of the pupal dry weight. The produced chitosan exhibited a spectrum of bioactivities, including antimicrobial, antioxidant, anti-inflammatory, and anticancer properties. These findings underscore the potential of insect-derived chitosan as a multifunctional biomaterial suitable for applications in biomedical, pharmaceutical, and environmental fields. Further studies could enhance its clinical translation and commercial scalability.

References

1. Dawwam, G, Al-Shemy, M., El-Demerdash, A. Green synthesis of cellulose nanocrystal/ZnO bio-nanocomposites exerting antibacterial activity and downregulating virulence toxigenic genes of food-poisoning bacteria. *Scientific Reports*, (2022), 12(1), 16848.

2. Zhou Y, Xu S, Zhang X, Zhou L, Zheng H, Zhu G. Recent advances of 5-endo-trig radical cyclization: promoting strategies and applications. Chem Commun. 2024;60:10098–111.

3. Pellis A, Guebitz GM, Nyanhongo GS. Chitosan: Sources, Processing and Modification Techniques. Gels. 2022;8:393.

4. Hamed I, Özogul F, Regenstein JM. Industrial applications of crustacean by-products (chitin, chitosan, and chitooligosaccharides): A review. Trends in Food Science & Technology. 2016;48:40–50.

5. Thambiliyagodage C, Jayanetti M, Mendis A, Ekanayake G, Liyanaarachchi H, Vigneswaran S. Recent Advances in Chitosan-Based Applications-A Review. Materials (Basel). 2023;16:2073.

6. Maliki S, Sharma G, Kumar A, Moral-Zamorano M, Moradi O, Baselga J, et al. Chitosan as a Tool for Sustainable Development: A Mini Review. Polymers (Basel). 2022;14:1475.

7. Raafat D, Sahl H-G. Chitosan and its antimicrobial potential--a critical literature survey. Microb Biotechnol. 2009;2:186–201.

8. Zhou J, Wen B, Xie H, Zhang C, Bai Y, Cao H, et al. Advances in the preparation and assessment of the biological activities of chitosan oligosaccharides with different structural characteristics. Food Funct. 2021;12:926–51.

9. Aranaz I, Alcántara AR, Civera MC, Arias C, Elorza B, Heras Caballero A, et al. Chitosan: An Overview of Its Properties and Applications. Polymers (Basel). 2021;13:3256.

10. Patrulea V, Ostafe V, Borchard G, Jordan O. Chitosan as a starting material for wound healing applications. Eur J Pharm Biopharm. 2015;97 Pt B:417–26.

11. Ibrahim MA, Alhalafi MH, Emam E-AM, Ibrahim H, Mosaad RM. A Review of Chitosan and Chitosan Nanofiber: Preparation, Characterization, and Its Potential Applications. Polymers. 2023;15:2820.

12. Kulka K, Sionkowska A. Chitosan Based Materials in Cosmetic Applications: A Review. Molecules. 2023;28:1817.

13. Muñoz-Tebar N, Pérez-Álvarez JA, Fernández-López J, Viuda-Martos M. Chitosan Edible Films and Coatings with Added Bioactive Compounds: Antibacterial and Antioxidant Properties and Their Application to Food Products: A Review. Polymers (Basel). 2023;15:396.

14. Soetemans L, Uyttebroek M, Bastiaens L. Characteristics of chitin extracted from black soldier fly in different life stages. Int J Biol Macromol. 2020;165 Pt B:3206–14.

15. Rodríguez JJG, Mirón AS, Camacho FG, García MCC, Belarbi EH, Chisti Y, et al. Causes of shear sensitivity of the toxic dinoflagellate protoceratium reticulatum. Biotechnology Progress. 2009;25:792–800.

16. Yuan B-Q, Yu T-H, Chen S-C, Zhang Z-Q, Guo Z-K, Huang G-X, et al. Physical and chemical characterization of chitin and chitosan extracted under different treatments from black soldier fly. Int J Biol Macromol. 2024;279 Pt 2:135228.

17. Korniienko V, Husak Y, Diedkova K, Varava Y, Grebnevs V, Pogorielova O, Pogorielov M. Antibacterial potential and biocompatibility of

chitosan/polycaprolactone nanofibrous membranes incorporated with silver nanoparticles. *Polymers*, 2024, *16*(12), 1729..

18. Brand-Williams W, Cuvelier ME, Berset C. Use of a free radical method to evaluate antioxidant activity. LWT - Food Science and Technology. 1995;28:25–30.

19. Miller NJ, Rice-Evans CA. The relative contributions of ascorbic acid and phenolic antioxidants to the total antioxidant activity of orange and apple fruit juices and blackcurrant drink. Food Chemistry. 1997;60:331–7.

20. Oyaizu M. Studies on Products of Browning Reaction. The Jap J Nut and Diet. 1986;44:307–15.

21. Gülçin I, Küfrevioglu OI, Oktay M, Büyükokuroglu ME. Antioxidant, antimicrobial, antiulcer and analgesic activities of nettle (Urtica dioica L.). J Ethnopharmacol. 2004;90:205–15.

22. Lo Scalzo R. EPR free radical scavenging activity on superoxide, hydroxyl and tert–butyl hydroperoxide radicals by common hydrophilic antioxidants: effect of mixing and influence of glucose and citric acid. Eur Food Res Technol. 2021;247:2253–65.

23. Adithya ES, Lakshmi MS, Hephzibah P, Sasikumar JM. In vitro antioxidant, anti-lipid peroxidation activities and HPLC analysis of methanol extracts from bark and stem of Mahonia leschenaultia takeda. Asian Journal of Plant Science and Research. 2013;3:116–26.

24. Lee G, Choi TW, Kim C, Nam D, Lee S-G, Jang H-J, et al. Anti-inflammatory activities of Reynoutria elliptica through suppression of mitogen-activated protein kinases and nuclear factor-κB activation pathways. Immunopharmacol Immunotoxicol. 2012;34:454–64.

25. Mosmann T. Rapid colorimetric assay for cellular growth and survival: application to proliferation and cytotoxicity assays. J Immunol Methods. 1983;65:55–63.

26. Machado SSN, Silva JBA da, Nascimento RQ, Lemos PVF, Assis D de J, Marcelino HR, et al. Insect residues as an alternative and promising source for the extraction of chitin and chitosan. Int J Biol Macromol. 2024;254 Pt 3:127773.

27. Pedrazzani C, Righi L, Vescovi F, Maistrello L, Caligiani A. Black soldier fly as a New chitin source: Extraction, purification and molecular/structural characterization. LWT. 2024;191:115618.

28. Sáenz-Mendoza A, Zamudio-Flores P, Tirado-Gallegos J, García-Anaya M, Rios C, Acosta-Muñiz C, et al. Insects as a potential source of chitin and chitosan: Physicochemical, morphological and structural characterization. -A review. Emirates Journal of Food and Agriculture. 2023;35:388–407.

29. Azmi N, Lock SSM, Berghuis NT, Sarwono A, Zahra NL, Rahman A, et al. Influence of synthesis approach and formulation on the physicochemical properties of chitin and chitosan from Black Soldier Fly. Results in Engineering. 2024;23:102401.

30. Jantzen da Silva Lucas A, Quadro Oreste E, Leão Gouveia Costa H, Martín López H, Dias Medeiros Saad C, Prentice C. Extraction, physicochemical characterization, and morphological properties of chitin and chitosan from cuticles of edible insects. Food Chem. 2021;343:128550.

31. Shin C-S, Kim D-Y, Shin W-S. Characterization of chitosan extracted from Mealworm Beetle (*Tenebrio molitor, Zophobas morio*) and Rhinoceros Beetle (*Allomyrina dichotoma*) and their antibacterial activities. International Journal of Biological Macromolecules. 2019;125:72–7.

32. Luo Q, Wang Y, Han Q, Ji L, Zhang H, Fei Z, et al. Comparison of the physicochemical, rheological, and morphologic properties of chitosan from four insects. Carbohydr Polym. 2019;209:266–75.

33. Ahmed H, Noyon MA, Uddin MdE, Rafid MM, Hosen EngrMS, Layek R. Development and Characterization of Chitosan-Based Antimicrobial Films: A Sustainable Alternative to Plastic Packaging. Cleaner Chemical Engineering. 2025;11:100157.

34. Głąb M, Kudłacik-Kramarczyk S, Drabczyk A, Guigou MD, Sobczak-Kupiec A, Mierzwiński D, et al. Multistep Chemical Processing of Crickets Leading to the Extraction of Chitosan Used for Synthesis of Polymer Drug Carriers. Materials (Basel). 2021;14:5070.

35. Sánchez-Machado DI, López-Cervantes J, Escárcega-Galaz AA, Campas-Baypoli ON, Martínez-Ibarra DM, Rascón-León S. Measurement of the degree of deacetylation in chitosan films by FTIR, 1H NMR and UV spectrophotometry. MethodsX. 2024;12:102583.

36. Triunfo M, Tafi E, Guarnieri A, Salvia R, Scieuzo C, Hahn T, et al. Characterization of chitin and chitosan derived from Hermetia illucens, a further step in a circular economy process. Sci Rep. 2022;12:6613.

37. Iber B, Kasan N, Torsabo D, Omuwa J. A Review of Various Sources of Chitin and Chitosan in Nature. JOURNAL OF RENEWABLE MATERIALS. 2021;10:42–9.

38. Sarhan A. Characterization of Chitosan and Polyethylene glycol Blend Film. Egyptian Journal of Chemistry. 2019;62 Special Issue (Part 2) Innovation in Chemistry:405–12.

39. Ke C-L, Deng F-S, Chuang C-Y, Lin C-H. Antimicrobial Actions and Applications of Chitosan. Polymers. 2021;13:904.

40. Sharif S, Abbas G, Hanif M, Bernkop-Schnürch A, Jalil A, Yaqoob M. Mucoadhesive micro-composites: Chitosan coated halloysite nanotubes for sustained drug delivery. Colloids and Surfaces B: Biointerfaces. 2019;184:110527.

41. Tsai G-J, Su W-H. Antibacterial Activity of Shrimp Chitosan against *Escherichia coli*. Journal of Food Protection. 1999;62:239–43.

42. Chung Y-C, Chen C-Y. Antibacterial characteristics and activity of acid-soluble chitosan. Bioresource Technology. 2008;99:2806–14.

43. Kim KW, Thomas RL. Antioxidative activity of chitosans with varying molecular weights. Food Chemistry. 2007;101:308–13.

44. Wen Z-S, Liu L-J, Qu Y-L, Ouyang X-K, Yang L-Y, Xu Z-R. Chitosan nanoparticles attenuate hydrogen peroxide-induced stress injury in mouse macrophage RAW264.7 cells. Mar Drugs. 2013;11:3582–600.

45. Ueno H, Yamada H, Tanaka I, Kaba N, Matsuura M, Okumura M, et al. Accelerating effects of chitosan for healing at early phase of experimental open wound in dogs. Biomaterials. 1999;20:1407–14.

46. Chávez de Paz LE, Resin A, Howard KA, Sutherland DS, Wejse PL. Antimicrobial effect of chitosan nanoparticles on streptococcus mutans biofilms. Appl Environ Microbiol. 2011;77:3892–5.

47. Adhikari HS, Yadav PN. Anticancer Activity of Chitosan, Chitosan Derivatives, and Their Mechanism of Action. Int J Biomater. 2018;2018:2952085.